MATHEMATICAL BIOSCIENCES
AND ENGINEERING
Volume **10**, Number **1**, February **2013**

doi:10.3934/mbe.2013.10.37

pp. **37–57**

DISTRIBUTED DELAYS IN A HYBRID MODEL OF TUMOR-IMMUNE SYSTEM INTERPLAY

Giulio Caravagna[1] and Alex Graudenzi

Department of Informatics, Systems and Communication
University of Milan Bicocca
Viale Sarca 336, I-20126 Milan, Italy

Alberto d'Onofrio[1]

Department of Experimental Oncology
European Institute of Oncology
Via Ripamonti 435, I-20141 Milan, Italy

Abstract. A tumor is kinetically characterized by the presence of multiple spatio-temporal scales in which its cells interplay with, for instance, endothelial cells or Immune system effectors, exchanging various chemical signals. By its nature, tumor growth is an ideal object of hybrid modeling where discrete stochastic processes model low-numbers entities, and mean-field equations model abundant chemical signals. Thus, we follow this approach to model tumor cells, effector cells and Interleukin-2, in order to capture the Immune surveillance effect.

We here present a hybrid model with a generic delay kernel accounting that, due to many complex phenomena such as chemical transportation and cellular differentiation, the tumor-induced recruitment of effectors exhibits a lag period. This model is a Stochastic Hybrid Automata and its semantics is a Piecewise Deterministic Markov process where a two-dimensional stochastic process is interlinked to a multi-dimensional mean-field system. We instantiate the model with two well-known weak and strong delay kernels and perform simulations by using an algorithm to generate trajectories of this process.

Via simulations and parametric sensitivity analysis techniques we (*i*) relate tumor mass growth with the two kernels, we (*ii*) measure the strength of the Immune surveillance in terms of probability distribution of the eradication times, and (*iii*) we prove, in the oscillatory regime, the existence of a stochastic bifurcation resulting in delay-induced tumor eradication.

1. **Introduction.** Tumor cells are characterized by a wide number of both genetic and epigenetic events, which induce the appearance of surface neo-antigens that may trigger the intervention of both the innate and the specific Immune System [64, 66]. So, in last two decades a number of evidences have accumulated [36] in support of Ehrlich's *Immune surveillance* hypothesis [37], i.e. that the Immune System may control the tumor growth and in some case also eliminate neoplasms.

The tumor-Immune system interplay is a very complex dynamical system and has, consequently, multiple outcomes. For example, tumors that are able to escape from the Immune control may in soem cases grow up to a large carrying capacity,

2010 *Mathematics Subject Classification.* 62P10, 92-08, 34A38, 65C05, 65L03.

Key words and phrases. Tumor, immune system, delay differential equation, Stochastic Hybrid Automata, piecewise deterministic Markov process, distributed delays.

1 Corresponding authors: giulio.caravagna@disco.unimib.it and alberto.donofrio@ieo.eu.

although usually the host organism dies well before that this large equilibrium is reached. In other cases, they may establish a dynamic equilibrium with the Immune system so that the tumor remains in a microscopic undetectable "dormant" steady-state [24]. They may also set in a oscillatory regime, which may be of two kinds: "short term-small amplitude" oscillations [53, 72, 43, 62] and patterns of remission-recurrence [69, 7, 68].

However, the above picture is incomplete since it does not take into account the fact that the Tumor-Immune system interaction is also evolutionary: the neoplasm may develop strategies to circumvent the Immune system action, thus restarting to grow [73, 64, 36, 70]. This phenomenon termed "immunoediting" [36], is remindful of an ecological adaptation [29, 30], and typically requires to complete a significant fraction of the average host life span [36]. Quite interestingly it might negatively impact on the effectiveness of immunotherapies [29].

As far as the mathematical modeling of tumor–Immune system interplay is concerned, many mean-field deterministic and stochastic models have appeared [55, 59, 58, 34, 24, 4, 28, 29, 30], some of them including delays [12, 71, 31].

Since the interaction of tumor cells with other kinds of cells - in our case Immune system effectors - also involves the exchange of a number of chemical signals, tumor-Immune system interplay is an ideal object of hybrid modeling where tumor and Immune system cells are represented by discrete stochastic processes, and chemical signals are modeled by mean-field equations [14, 27]. Thus, considering the *intrinsic noise* of the model may allow for more informative forecasts than in the case of a men-field based model [14].

In [14, 27] we proposed a hybrid version of the well-known Panetta-Kirschner [55] mean-field model of the interlinked dynamics of tumor cells, effector cells and Interleukins-2. The original model reproduces various kinds of biological phenomena, including tumor size oscillations [53, 72, 43, 62, 68, 69], as well as growth up to a carrying capacity or tumor dormancy. However it is unable to capture tumor elimination by the Immune system. On the contrary this phenomenon is fully captured by the hybrid model of [14], which was extended in [27] to account for both interleukin-based therapies and Adoptive Cellular Immunotherapies, i.e. the transfusion of autologous or allogeneic T cells into tumor-bearing hosts [51], and model outcomes have been investigated under various therapeutic settings.

However, the above hybrid model did not take into account that the influence of tumor size on the dynamics of effectors is not instantaneous since it is the result of both transport of intercellular signaling and the maturation and activation of T-lymphocytes mediated by B-lymphocytes [41, 65]. These and other phenomena [41, 65] induce a remarkable lag period that must be taken into the account when modeling the immuno-oncological processes.

Having this in mind, here we couple the mean-field equation for Interleukins-2 with a bi-dimensional delayed stochastic process. For the sake of the precision the stochastic process will have a component that is not directly affected by the lag, namely the dynamics of tumor cells, and a component that is directly affected, namely the dynamics of the population of Immune effectors. The introduction of the delay heuristically approximates the missing dynamical components. As we shall see, despite the adopted abstraction being a highly macroscopic and simplistic representation of tumor-Immune system interplay, it can still provide useful insights in its understanding. Also, this new hybrid system with delay is a Piecewise Deterministic Markov stochastic process [32, 9, 10]. As a consequence, numerical

realizations of the model are obtained by generalizing the Gillespie-like Stochastic Simulation Algorithm defined for the delay-free hybrid system in [14].

As far as the delay is concerned, in the mean-field literature two approaches have been followed [56, 39]. The first consisting in the representation of the delay as a simple constant deviation in the argument of some state variables [56, 57]. This approach has a great historical and mathematical relevance. However, from a physical point of view it may only deemed acceptable in the case of the delay being a random variable very narrowly distributed around its mean value, i.e. when the ratio between the standard deviation of the delay over its mean value is sufficiently small. Note that in such a case the density of the delay can be fairly approximated by a Dirac's delta function centered at its mean value.

The second approach consists in considering distributed delays [56, 39], i.e. delays whose density is a regular bounded positive function, with unitary L_1 norm, of course. This approach, which allows to more closely mimic the reality, leads to integro-differential systems, where the integral part derives form taking into account the distributed nature of the delay. The density of the delay is called *delay kernel*. The constant delay case, thus, may be considered a limit case of a distributed delay, where the delay kernel is a Dirac's delta function.

Both the above classes of delay-differential equations have an infinite-dimensional state space [56, 39], as it may easily seen by considering their solution requires the knowledge of the delayed state variables in a past interval $[t_0-\tau_{max}, t_0]$, where τ_{max} is the maximum considered delay and t_0 an initial time. In other words, one has to know these variables in a infinite number of points. Note that there are classes of delay kernel that allow to reduce the integral part of the integro-differential system to a finite number of supplementary *ordinary differential equations* (ODEs) [56, 39].

In our hybrid model we shall follow the second approach. After setting our problem in general framework with a general delay kernel, we shall particularize our study the Erlangian kernels that allows the above-mentioned reduction to finite dimensions.

The structure of this paper is the following: in Section 2 some background and the delayed model is presented, with complete details on its formulation in terms of hybrid automata and the underlying stochastic processes; algorithms for the realization of such processes are discussed in Section 3; the results of our numerical simulations are discussed in Section 4. Concluding remarks conclude this work.

2. **Model definition.**

We start by recalling the model introduced in [55]. Two cell populations, i.e. tumor cells T and Immune system effectors E, and the molecular population of Interleukins-2 (IL-2) I are considered. The hybrid model consists of two equations for cells

$$T' = rT\left(1-\frac{b}{V}T\right) - \frac{p_T T}{g_T V + T}E \qquad E' = \frac{p_E I}{g_E + I}E - \mu_E E + cT \tag{1}$$

and one equation for ILs-2, that is

$$I' = \frac{p_I}{V}\frac{TE}{g_I V + T} - \mu_I I\,. \tag{2}$$

Cells equations are obtained converting into exact numbers the densities T_* and E_* of the analogous mean-field model of the ref. [27], i.e. $T_* = T/V$ and $E_* = E/V$ where V is the volume. Here the tumor induces the recruitment of the effectors at a linear rate $cT(t)$. Also, c is a measure of the immunogenicity of the tumor, i.e. c is "a

measure of how different the tumor is from self" [55]. Biologically, c corresponds to the average number of antigens expressed by each tumor cell. Interleukins stimulate effectors proliferation, whose average lifespan is μ_E^{-1}, and the average degradation time for IL-2 is μ_I^{-1}. The source of interleukin is modeled as linearly depending on both E and the T. Michaelis-Menten kinetics rules IL-2 production by the tumor Immune-system interplay, effectors recruitment by their interplay with IL-2 and effectors-induced tumour death. Finally, tumor growth is modeled with a logistic curve with a plateau $1/b$. In [14] it is shown that this model predicts a desired *tumor eradication via Immune surveillance*, whereas the mean-field analogous does not [55]. Adoptive Cellular Immunotherapies and Interleukin-based therapies have been added to the model in [27], and the effectiveness of impulsive and piece-wise constant infusion delivery scheduling investigated.

The advantage of employ a hybrid model with respect to a deterministic one is that the hybrid setting allows capturing events such as the tumor eradication, which cannot be forecasted in the deterministic case. This allows us to compute the probability of eradication, i.e. $\mathcal{P}[T(t) = 0]$ for some t, given various model configurations. These quantities can be interpreted as a measure of the strength of the Immune surveillance.

Here we consider the case where the effect of the tumor-driven stimulation of the Immune system is neither instantaneous nor deterministically delayed, but instead it is affected by a delay, whose distribution is given by a general probability density $K(x)$ where $\int_0^{+\infty} K(x)dx = 1$. Thus, in a general kernel equation (1) reads as

$$E' = \frac{p_E I}{g_E + I} E - \mu_E E + cZ(t)\,, \tag{3}$$

where a further deterministic variable Z is introduced, whose dynamics is given by

$$Z(t) = \int_0^{+\infty} T(t-x)K(x)dx\ . \tag{4}$$

Differently from [14], where $\{(T(t), E(t))\}$ is a stochastic process interlinked to a linear scalar ODE with randomly varying coefficients describing $I(t)$, here we have a further integral equation describing the dynamics of the delayed variable Z.
The general case is quite difficult do deal with. Thus, here we shall assume that the delay kernel $K(x)$ belongs to a family of probability distribution with a prominent role in the theory of dynamical systems with delays, namely the *Erlang family*

$$\mathrm{Erl}_M(t) \quad = \quad \frac{a}{(M-1)!}(at)^{M-1}e^{-at}\,. \tag{5}$$

The Erlang distribution generalizes the exponential distribution, i.e. for $M = 1$ it is exponential, the average delay is $\theta = M/a$ and its standard deviation is $\sigma = \theta/\sqrt{M}$. We also remark that for $M \to +\infty$ the Erlang converges to a Dirac distribution.

The Erlang distribution has a noteworthy property: the integral equation for $Z(t)$ is equivalent to an additional linear ODE system. Indeed, defining the vector of additive state variables $\mathbf{W} = (W_1(t), \ldots, W_M(t))$, and considering the following M-dimensional linear differential system

$$\begin{cases} W_1'(t) = a(T(t) - W_1(t)) \\ \qquad\qquad \cdots \\ W_M'(t) = a(W_{M-1}(t) - W_M(t)) \end{cases} \tag{6}$$

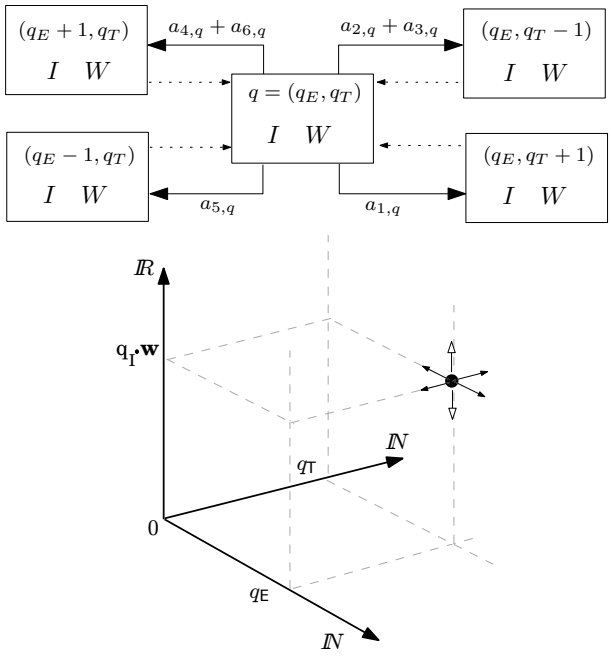

FIGURE 1. **SHA and state space of its underlying PDMP.** In top we draw mode $q = (q_T, q_E)$ with its outgoing transition and part of of the incoming ones. In bottom we plot the state space $\mathbb{N} \times \mathbb{N} \times \mathbb{R}_+^{M+1}$ for the PDMP [32] underlying the hybrid model with M-dimensional Erlang kernel. Once the process enters state $(q_T, q_E, q_I \cdot \mathbf{w})$ the only movement gradient is on the z-axis, i.e. the horizontal component (q_T, q_E) is fixed and the process moves according to the vertical vector field, denoted by the empty arrows, determining $I(t)$ and $\mathbf{W}(t)$. The process persists moving according to equation (9), and then moves on the $\mathbb{N} \times \mathbb{N}$ sub-space, i.e. the horizontal discrete grid denoted by the full arrows, according to equation (10).

one can show that

$$Z(t) = W_M(t)\,. \tag{7}$$

Note that by defining the matrix $A \subseteq \mathbb{R}^{M\times M}$ as $A_{i,i} = -a$, and, for $i > 1$, as $A_{i,i-1} = a$, and 0 elsewhere, and by defining the transpose vector $\mathbf{u} = (1, 0, \ldots, 0)$ one may write system (6) in the compact notation $\mathbf{W}'(t) = A\mathbf{W}(t) + aT(t)\mathbf{u}$. It is useful to define the row vector $\mathbf{p} = (0, \ldots, 1)$, so that $Z(t) = \mathbf{p}\mathbf{W}(t)$. The additional system (6) is again a linear differential equation, although vectorial, with random coefficients, actually constant in the intervals between two consecutive stochastic events.

This model is a *Stochastic Hybrid Automaton* (SHA, [9, 10]) with modes in $\mathbb{N}\times\mathbb{N}$ recording cellular concentrations. This SHA is an extension of the one for the delay-free case [14]. The SHA consists of a mode for each possible value of E and T, i.e. a mode $q = (q_E, q_T)$ to count q_e and q_T effector and tumor cells, with inside the

vector fields of equation (2) and equation (4), i.e. such a mode contains

$$\begin{cases} I(t) = B_q + (I_q - B_q)\exp\Big(-\mu_I(t-t_q)\Big) \\ \mathbf{W}(t) = q_T\mathbf{h} + e^{A(t-t_q)}(\mathbf{w}_q - q_T\mathbf{h})\,, \end{cases} \tag{8}$$

where $\mathbf{h} = (1,\dots,1)$ is a row vector, $I(t_q) = I_q$ and $\mathbf{W}(t_q) = \mathbf{w}_q$ are initial conditions at the mode entrance time t_q and

$$B_q = \left(\frac{p_I q_T q_E}{g_I V^2 + q_T V}\right)\frac{1}{\mu_I}\,.$$

The automata execution switches probabilistically between modes, while continuous paths of $I(t)$, $\mathbf{W}(t)$ and, consequently, $Z(t) = W_M(t)$ are determined. When the automata jumps, at time t_q, from mode q to mode q', at time $t_{q'}$, the initial condition of I (resp. $\mathbf{W}$), i.e. $I(t_{q'})$ (resp. $\mathbf{W}(t_{q'})$), is set equal to the last evaluation of I, i.e. $I(t_q)$ (resp. $\mathbf{W}(t_q)$). Jumps between modes are determined by the time-inhomogenous stochastic events, i.e. the jump rates triggering changes in E and T depend on $I(t)$ and $Z(t)$ [14, 15]. The exit times for mode q are given by the time-dependent cumulative distribution function [15]

$$\mathcal{P}_q[\tau] = \exp\left(\sum_i \int_0^\tau a_{i,q}(t_q + t)dt\right) \tag{9}$$

and the probability of jumping to mode q', given the exit time τ, is

$$\mathcal{P}_q[q' \mid \tau] = \begin{cases} \dfrac{\sum_{j\in Q} a_{j,q}(t_q+\tau)}{\sum_i a_{i,q}(t_q+\tau)} & \text{if } Q = \{j \mid q + \nu_j = q'\} \\ 0 & \text{otherwise}\,. \end{cases} \tag{10}$$

Stochastic events $a_{2,q}$ and $a_{3,q}$ trigger jumps to the same new mode, i.e. jumps from $q = (q_E, q_T)$ to $(q_E - 1, q_T)$, so their probabilities are joined in Q. Here the Gillespie-like [44] notation is used so ν_j is the j-th column of the system *stoichiometry matrix*

$$\nu = \begin{pmatrix} 1 & -1 & -1 & 0 & 0 & 0 \\ 0 & 0 & 0 & 1 & -1 & 1 \end{pmatrix}$$

and the jump rates in $q = (q_T, q_E)$ are the time-dependet *propensity functions* [45]

$$\begin{aligned} &a_{1,q}(t) = r_2 q_T && a_{2,q}(t) = r_2 b V^{-1} q_T(q_T - 1) \\ &a_{3,q}(t) = (p_T q_T q_E)/(g_T V + q_T) && a_{4,q}(t) = [p_E q_E I(t)]/[g_E + I(t)] \\ &a_{5,q}(t) = \mu_E q_E && a_{6,q}(t) = cZ(t)\,. \end{aligned} \tag{11}$$

Notice that all but $a_{4,q}$ and $a_{6,q}$ are time-homogenous jump rates depending only on constants, rather than the deterministic flows. The overall underlying stochastic process is not homogenous, as in [14, 15]. In top panel of Figure 1 we graphically represent mode $q = (q_T, q_E)$ with its outgoing transition and part of of the incoming ones.

Executions of this SHA are also trajectories of the underlying *Piecewise Deterministic Markov Process* (PDMP) [32]. This very general stochastic jump process flows deterministically over a vector field and generates left-continuous paths triggered by (*i*) hitting user-defined boundaries of the state space and (*ii*) time-inhoumogenous jump distributions, which are actually linked to the vector field. For this case, the underlying PDMP has no hitting boundaries but only time-dependent jump rates linked to the vector field composed by the flows for $I(t)$ and $\mathbf{W}(t)$. The state space for the PDMP is $\mathbb{N}\times\mathbb{N}\times\mathbb{R}_+^{M+1}$, as shown in lower panel of Figure 1.

Algorithm 1 SSA [45] with time-dependent propensity functions to realize trajectories of the PDMP [32] underlying the Stochastic Hybrid Automata.

1: **Input:** state $(T_0, E_0, I_0, \mathbf{w}_0)$, start time t_0, stop time t_{stop};
2: set initial mode $q \leftarrow (q_{T_0}, q_{E_0})$ and set $I(t_0) = I_0$, $Z(t_0) = \mathbf{w}_0$;
3: **while** $t < t_{stop}$ **do**
4: let $r_1 \sim U[0,1]$ determine the mode exit time τ as $\mathcal{P}_q[\tau] = 1/r_1$ according to equation (12), jointly solve $I(t)$ and $Z(t)$ according to equations (7–8);
5: determine the jump rates $a_{j,q}(t+\tau)$, set $I(t+\tau)$ and $Z(t+\tau)$;
6: jump to mode q' with probability $\mathcal{P}_q[q' \mid \tau]$;
7: **end while**

In there, once the process enters state $(q_T, q_E, q_I \cdot \mathbf{w})$ the only movement gradient is on the z-axis, i.e. the horizontal component (q_T, q_E) is fixed and the process moves according to the vertical vector field. The process persists moving according to equation (9), and then moves on the $\mathbb{N} \times \mathbb{N}$ sub-space, i.e. the horizontal discrete grid, according to equation (10).

3. **Model simulation.** We present here an algorithm to realize trajectories of the the underlying PDMP, an extension of the algorithm presented in [14]. Algorithm 1, is based on the Gillespie *Stochastic Simulation Algorithm* (SSA) [44, 45] accounting for time-dependent jump rates.

The algorithm works by determining, at each iteration, both the exit time from the current mode and the next mode. So, when at time t_q the automaton enters a mode q, the exit time τ (see step 4) is determined by the parallel solution of $I(t)$ and $Z(t)$, $t \geq t_q$, and $\mathcal{P}_q[\tau]$ as triggered by the jump rates $a_{j,q}(t)$. As in [14], samples from $\mathcal{P}_q[\tau]$ are obtained by a unit-rate Poisson transformation, i.e.

$$\sum_i \int_0^\tau a_{i,q}(t_q + t)dt = \ln\left(\frac{1}{r_1}\right) \tag{12}$$

with r_1 uniformly distributed.

Once the jump time is determined, the new mode is chosen by a weighted probabilistic choice depending on $a_{i,q}(t+\tau)$, i.e.

$$j = \min\left\{ n \;\middle|\; r_2 \cdot a_0(\mathbf{x}, t+\tau) \leq \sum_{i=1}^{n} a_i(\mathbf{x}, t+\tau) \right\} \tag{13}$$

with r_2 uniformly distributed and $a_0(\mathbf{x}, t+\tau) = \sum_{i=1}^{M} a_{i,q}(t+\tau)$. Algorithm 1 iteratively performs a realization of the PDMP by starting from an initial configuration $(T_0, E_0, I_0, \mathbf{w}_0)$. In Appendix A further comments on this algorithm are discussed.

3.1. **Weak and strong kernels.** Among the wide family of the Erlang kernels, we focus on two well known ones: the *weak* and *strong* delay kernels [39]. These kernels are successfully applied in many fields of theoretical biology: epidemiology [8], behavioral epidemiology [25], ecology of prey predator systems [5, 75, 39], stem cells proliferation [20], dynamics of neural networks [49, 50], theoretical population biology [67, 48], immunology of infections [26] and systems biology [40].

The former is defined for $M = 1$, i.e. it is an exponential distribution

$$K_{\text{weak}}(t) = ae^{-at},$$

whereas the latter is defined for $M = 2$ as

$$K_{\text{strong}}(t) = a^2 t e^{-at}\,.$$

By considering that if $M = 1$ then $a = 1/\theta$, whereas if $M = 2$ then $a = 2/\theta$, further simplifications of the PDMP jump equation (12) are possible, as discussed in Appendix B.

3.2. **Kinetic parameters.** For the sake of comparing the effect of the above mentioned kernels on the interplay outcome, we use the same values of the model parameters used in the determinsitic works by D. Kirschener and coworkers [55, 54]. The baseline growth rate of the tumor is $r = 0.18\,days^{-1}$ and the organism carrying capacity is $b = 1/10^9\,ml^{-1}$. The baseline strength of the killing rate of tumor cells by E, of the $IL-2$-stimulated growth rate of E and of the production rate for I are, respectively, $p_T = 1\,ml/days$, $p_E = 0.1245\,days^{-1}$ and $p_I = 5\,pg/days$. The corresponding 50% reduction factors are $g_T = 10^5\,ml^{-1}$, $g_E = 2 \cdot 10^7\,pg/l$ and $g_I = 10^3\,ml^{-1}$, respectively. The degradation rates are $\mu_E = 0.03\,days^{-1}$ for the inverse of the average lifespan of E and $\mu_I = 10\,days^{-1}$ for the loss/degradation rate of IL_2. Finally, the reference volume is $V = 3.2\,ml$.

These values pertain to mice [54, 55], which utilized various works appeared in experimental biophysics literature on tumor kinetics, for example [33, 59], where some accurate fitting of real data concerning laboratory animals were performed. Volume V, instead, has adopted in [14] by considering the average blood volume of a chimeric mouse. The value of θ and c are varied in each configuration.

4. **Results.** With the purpose of investigating the effect of different delay kernels, and of different values of the average dealy θ, on the tumor eradication time, if any, and on the tumor growth size, we performed extensive simulations of various model configurations. All the simulations have been performed by a JAVA implementation of the model; simulation times decrease as T and E increase in size, spanning from few minutes to some hours.

We always used the initial condition $(T_0, E_0, I_0, \mathbf{w}_0) = (1, 0, 0, 0)$ [14].

4.1. **The eradication regime.** For $c = 0.02$, a value used in Figure 2 of [14], we used $\theta \in \{0, 0.5, 1, 1.5, 2, 2.5, 3\}$ *days* since, for $\theta > 3$, it is shown in [31] that the tumor mass grows up to the carrying capacity of the organism, i.e. $1/b$. We remark that $\theta > 3$ is biologically unrealistic [31]. We performed 10^3 simulations for each delay configuration, and we plot the averages tumor and effectors growth, i.e. $\langle T(t)\rangle$ and $\langle E(t)\rangle$, in Figure 2. In there, we show both weak and strong kernels.

Looking at Figure 2 one can notice that the average number of tumor cells $\langle T(t)\rangle$ grows faster and up to larger maximum values in correspondence of higher magnitudes of the delay, for both the weak and the strong kernel, even if for each delay value the model still predicts tumor eradication. Analogously, this relation is maintained also with respect to the average number of effector cells $\langle E(t)\rangle$. Furthermore, for the same value of delay, both the maximum value and the overall number computed on the whole simulation time of both the tumor and the effector cells are larger in the strong kernel case than in the weak kernel one. The differences in the magnitude of the variables are indeed remarkable, e.g. in the case of no delay ($\theta = 0$) the tumor cells reach an average maximum value of around 10^6, while for the highest considered delay - i.e. $\theta = 3$ - this value is 4 times bigger in the case of weak kernel and almost 5 times bigger in the case of strong kernel. We also remark

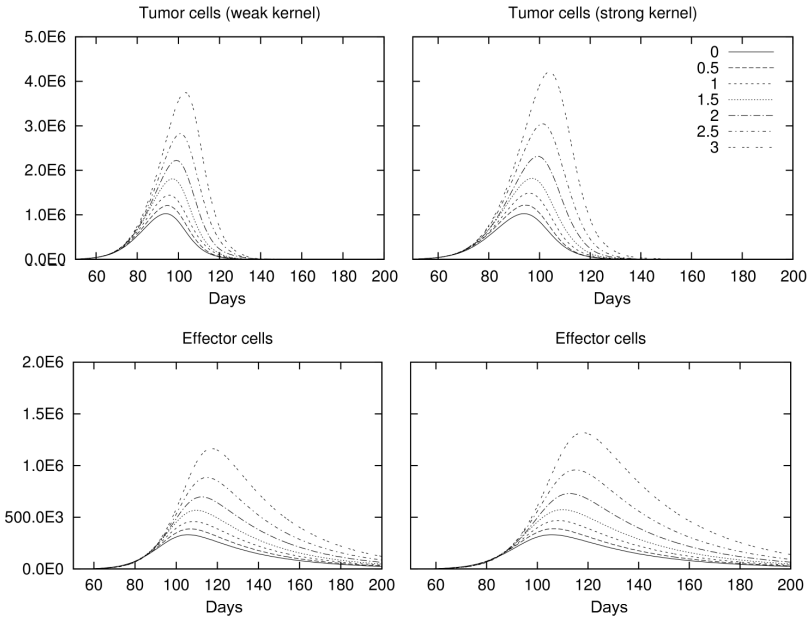

FIGURE 2. **Tumor and Effectors growth.** We plot the average growth $\langle T(t)\rangle$ and $\langle E(t)\rangle$ as of 10^3 simulations with $c = 0.02$, $\theta \in \{0, 0.5, 1, 1.5, 2, 2.5, 3\}$ and $(T_0, E_0, I_0) = (1, 0, 0)$. We compare the delay-free model, the weak ($M = 1$) and the strong kernel ($M = 2$). Days and number of cells are represented on the axis.

that the average peaks for both the tumor and the effector cells are reached slightly later in time for larger values of delays.

In Figure 3 we can observe the probability densities of the tumor eradication time, i.e. $\mathcal{P}[T(t) = 0]$. Interestingly, the peaks of the curves concerning both the strong and the weak kernel are observed in very similar moment in time -i.e. around 115 days - for all the considered values of delay and significantly sooner than the peak regarding the model with no delay, i.e. around 125 days. We can hypothesize that, even though larger values of delays imply a larger and faster growth of the tumor mass, the Immune system reacts in a more efficient way and, as a consequence, the tumor eradicates quicker. This not expected result clearly points at the important role of delays in controlling tumor expansion.

4.2. **Parametric sensitivity analysis.** We used a *parametric sensitivity analysis* (PSA,[22]) technique to quantitatively characterize the influence that a variation of the delay value has on the number of tumor cells, within the eradication regime. This PSA technique was firstly introduced to detect the influence of arbitrary large variations of a key input parameter (θ in our case) on the overall probability distribution of an output variable ($\mathcal{P}[T(t)]$ in our case). Other approaches, instead, consider aggregate model variables such as the distribution mean [18].

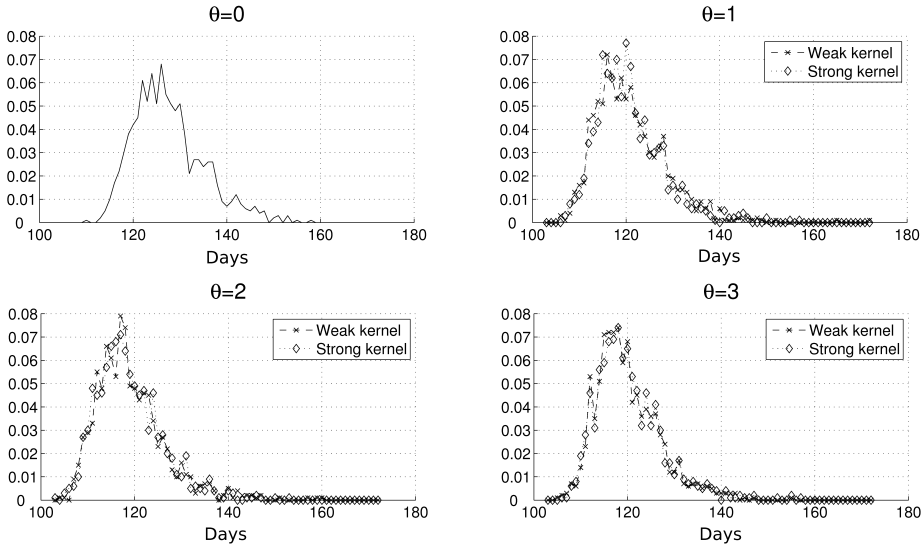

FIGURE 3. **Tumor eradication time probabilities.** We plot in the left panel the empirical probability density of the tumor eradication time, i.e. $\mathcal{P}[T(t) = 0]$ with $t \in \mathbb{N}$, for $c = 0.02$, $(T_0, E_0, I_0, \mathbf{w}_0) = (1, 0, 0, 0)$ and four values of delay $\theta \in \{0, 1, 2, 3\}$. We compare the delay-free model, the weak ($M = 1$) and the strong kernel ($M = 2$).

In this PSA the model sensitivity to θ is defined as a function of the θ itself. In detail, the sensitivity of $\mathcal{P}[T(t)]$ as a function of time and θ is defined as [47]

$$S_T(t, \theta) = \int_{\mathbb{N}} \left| \frac{\partial \mathcal{P}_\theta[T(t) = x]}{\partial \theta} \right| \mathcal{P}_\theta[T(t) = x] dx \,. \tag{14}$$

where $\mathcal{P}_\theta[T(t)]$ is the probability of the number of tumor cells, given a value of θ and $\mathbb{N}$ is the domain of integration of x: we are indeed considering the discrete part of the PDMP. Notice that $\mathcal{P}_\theta[T(t) = x]$ is the solution of the master equation of the model for a given θ and that we consider the normalized sensitivity values by multiplying for $\mathcal{P}_\theta[T(t) = x]$.

The sensitivity of the model with respect to any value of time and θ is so given by a Lagrange interpolation of the various $S_T(t, \theta)$, by means a polynome of order $D-1$, being D the number of distinct considered delays, see the left panel in Figure 4. We remark that this technique is particularly useful here because, by considering distinct delay kernels, our goal is to understand whether the system may be more or less sensitive to variations of the delay in some region of the parameter's space.

Finally, we restrict the sensitivity measure to time by defining

$$S_T(t) = \int_{\Omega\theta} S_T(t, \theta) d\theta \tag{15}$$

where the finite domain $\Omega\theta = \{0.1\, k \mid 0 \leq k \leq 30, k \in \mathbb{N}\}$ for θ is used. The resulting curve intuitively represents the area below the 3D curves in Figure 4, and it is evaluated by performing 10^3 simulations for each value of θ.

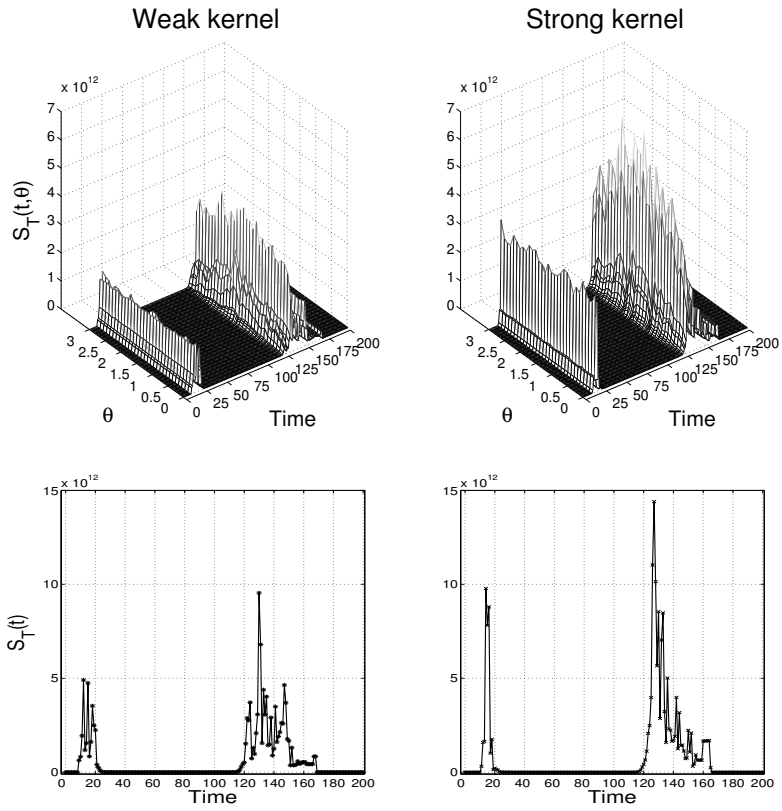

FIGURE 4. **Parametric sensitivity analysis.** In top panels the 3-D representation of the sensitivity curves $S_T(t,\theta)$, plotted for each delay $\theta = 0.1\,k$ ($0 \leq k \leq 30$, $k \in \mathbb{N}$), and $t \in [0, 200]$ as from equation (14). These are obtained by 3×10^5 independent simulations, for the weak (left plots) and the right kernel (right plots). In bottom panels we plot the corresponding sensitivity curves $S_T(t)$ as from equation (15).

Looking at Figure 4, one can immediately notice that, despite a significant difference in the magnitude, both kernels display a profoundly similar behaviour. In particular, the system appears to be highly sensitive to variations of the delay only in two circumscribed regions, i.e. in the intervals $[10, 25]$ and $[115, 165]$, while in the other regions it seems to be almost insensitive. Besides, the height of the second peak doubles the first peak in the weak kernel and is 50% larger in the strong kernel. This outcome firstly points at the importance of defining the sensitivity as a function of time, as we deal with a complex dynamical system whose behaviour can deeply variate in course of time.

One possible explanation of this result is related to the dynamical properties of system: the variation of the speed of the Immune response, which clearly depends on the magnitude of the delay, strongly influences tumor expansion, either favoring or contrasting it. This only if the tumor is still in its preliminary phase, i.e. the first

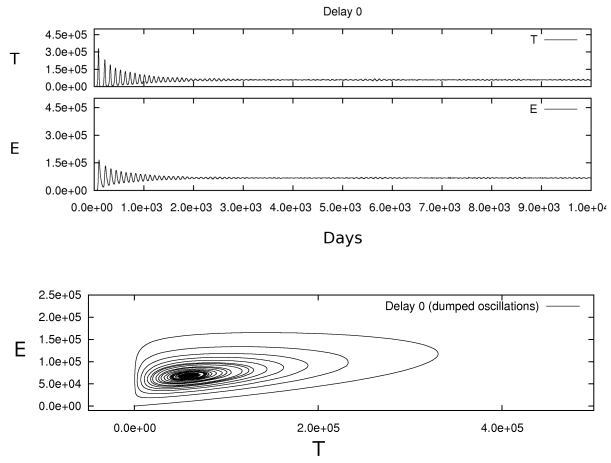

FIGURE 5. **Dumped oscillations in the delay-free case.** We plot the variation in time of $T(t)$ (first row) and $E(t)$ (second row) for a single run with $c = 0.035$ and $\theta = 0$. The initial configuration is $(T_0, E_0, I_0) = (1, 0, 0)$. On the x-axis days are represented, on the y-axis number of cells. In third row we plot the phase space of the system restricted to T (y-axis) and E (x-axis).

peak, or has reached its maximum size, i.e. the second peak, while in the Immune suppression phase it is substantially not influential.

Furthermore, by examining $S_T(t, \theta)$ (3D plots) it turns out that in both cases the sensitivity curves in correspondence of the second peak is bell shaped. This means that an identical variation of θ starting from distinct baseline values can indeed provoke distinct repercussions on the output of the model.

Finally, we highlight the considerable difference in magnitude with regard to the two distinct kernels, being the strong kernel model highly more sensitive than the weak kernel one, at least with respect to the relevant intervals. This phenomenon could be due to intrinsic nature of the considered delays. Given that the effect of the strong kernel-related delays on the dynamics of the system is, on average, more intense that that induced by weak kernel ones, so is the sensitivity of the system to their variations.

4.3. **The oscillatory regime.** In order to investigate the role of delays for the system in the oscillatory regime, we performed simulations with $0.03 \leq c \leq 0.035$, a region for which both the deterministic system [55] and the therapy-free hybrid model [14] predict tumor sustained or dumped oscillations. We compare the effect of the delay kernels in the oscillatory regime for $c = 0.035$, $\theta = 1.5$ and initial configuration $(T_0, E_0, I_0, \mathbf{w}_0) = (1, 0, 0, 0)$ (Fig. 6) against the delay-free case, as sown in Fig. 5. Here we simulate the model for around 27 years, i.e. 10^5 time units, a value far beyond the life expectancy of a mouse – on which parameters are fitted – but which serves mainly to prove the stability of the attractor, if any.

One can note that, while in the delay-free case the tumor mass tends to a unique asymptotic value, for $\theta = 1.5$ and for both the kernels, the dynamics apparently ends up in stochastic sustained oscillations. In particular, while in the delay-free

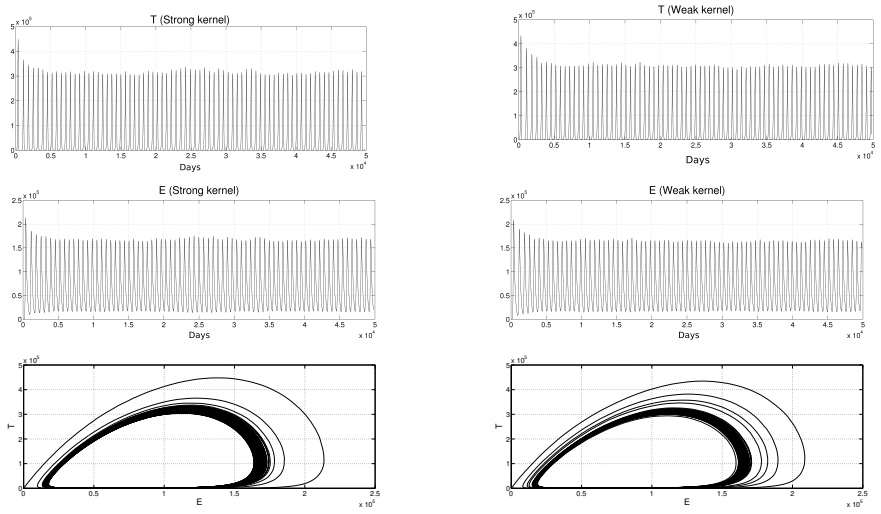

FIGURE 6. **Effect of weak and strong delay kernels on stable oscillatory attractors.** We plot the variation in time of $T(t)$ (first row) and $E(t)$ (second row) for a single run with $c = 0.035$ and $\theta = 1.5$, with regard to the strong (left) and the weak kernel (right). The initial configuration is $(T_0, E_0, I_0) = (1, 0, 0)$. On the x-axis days are represented, on the y-axis number of cells. In third row we plot the phase space of the system restricted to T (y-axis) and E (x-axis), for the strong (left) and the weak kernel (right).

case the oscillations are dumped up to an equilibrium value of around 10^5 cells, for both the kernels and $\theta = 1.5$, the values of T periodically range from around 0 and around 3×10^5, the peak being around 4.5×10^5. In the bottom plot in Fig. 5 we display the phase space of the system only considering T and E. We remark that in [63, 61, 60] it is shown that amplified oscillations may indeed appear as a consequence of the introduction of delays. It is also important to notice that no significant differences are detectable between the weak and the strong kernel case, with regard to the properties of the oscillations.

An interesting correlated phenomenon is then observed, that is the eradication of the tumor in a relevant number of cases. While in the delay-free case none of 1000 simulations led to the eradication of the tumor, in 140 and 204 simulations out of 1000 for, respectively, the weak and the strong kernel case with $\theta = 1.5$ the eradication was actually observed, usually just after the first oscillation. This outcome points at the existence of a stochastic bifurcation close to $\theta = 1.5$, in which a switch from the limit cycle to the null attractor $T \to 0$ is indeed possible. In Figure 7 one can observe the empirical probability density of the eradication time, i.e. $\mathcal{P}[T(t) = 0]$ with $t \in \mathbb{N}$, for both the weak and the strong kernel case. Also in this case, we do not detect remarkable differences between the two cases and this hints at a rather similar influence of the two distinct delay kernels on the overall dynamics.

In order to quantify the strength of the null attractor we also plot in Figure 7 the probability of switching to the attractor against the delay value. In there we

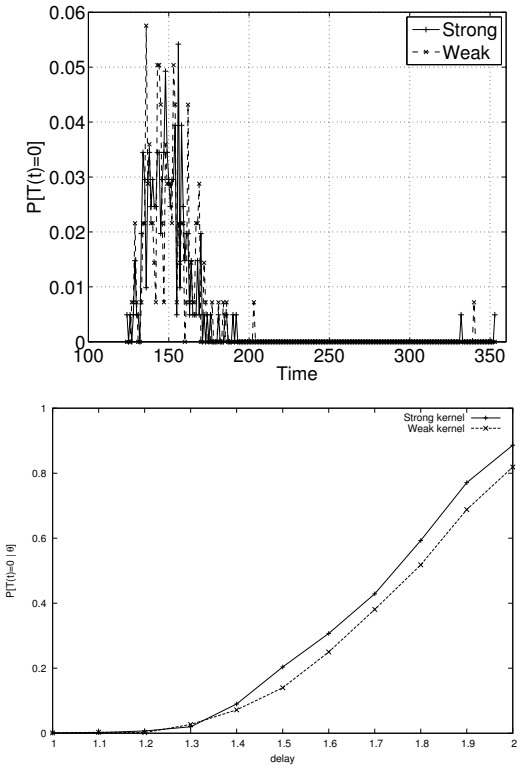

FIGURE 7. **Stochastic bifurcation for $\theta = 1.5$.** In top panel we plot the empirical probability density of the eradication time, i.e. $\mathcal{P}[T(t) = 0]$ with $t \in \mathbb{N}$, for $c = 0.035$, $\theta = 1.5$ and $(T_0, E_0, I_0, \mathbf{w}_0) = (1, 0, 0, 0)$, for both kernels. This probability is evaluated by the 140 (weak kernel) and 204 (strong kernel) cases, out of 1000, in which the system jumps to the null attractor. In bottom panel we quantify the probability of switching to the attractor $\mathcal{P}[T(t) = 0|\theta]$ against the delay value, for both kernels.

use $\theta \in [1, 2]$ and we show both kernels; this plot is obtained by discretizing θ every 0.1 units, and performing 1000 simulations for each kernel and for each delay.

The above illustrated outcome of our hybrid model is deeply different from that of the original mean-field model, for both types of kernels. Namely, in Figure 8 we show deterministic simulations of model with weak delay kernel, shown in left panels, and also with strong delay kernel, shown in right panels. In both cases we considered $\theta \in \{0, 0.5, 1, 1.5, 2, 2.5, 3\}$, and the system was simuated up to day 400. The initial condition was

$$T(t) = \begin{cases} 0 & t < 0 \\ 1 & t = 0 \end{cases}, \qquad E_0 = I_0 = 0\,,$$

thus leading to $W_1(0) = 0$ in the linear system (6) for the weak kernel, and to $W_1(0) = W_2(0) = 0$ for the strong kernel. It is of interest to notice that, although the structure of the two kernels are quite different, the plots are very similar.

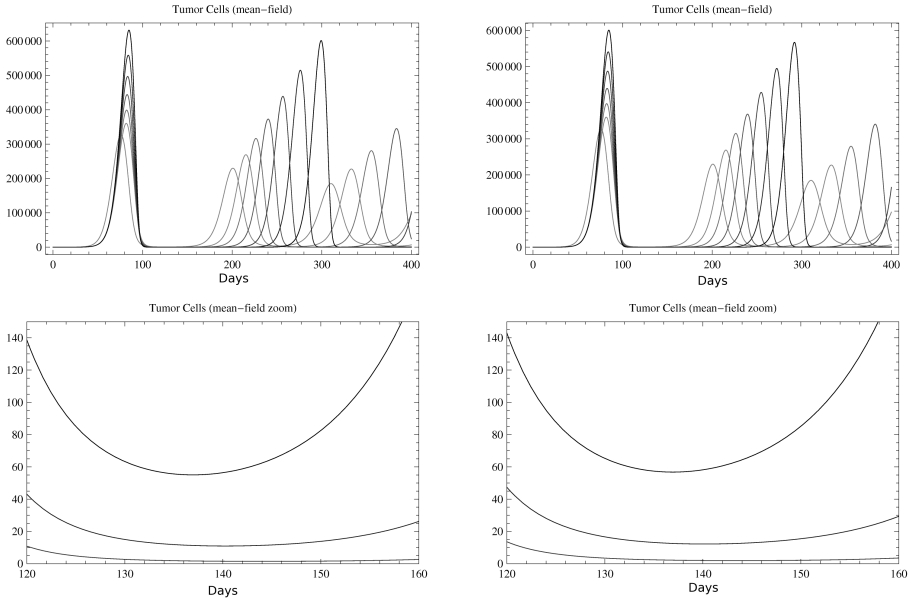

FIGURE 8. **Mean-field model.** We plot deterministic simulations of model (1-2) for $c = 0.035$, $\theta \in \{0, 0.5, 1, 1.5, 2, 2.5, 3\}$ (higher peaks for higher values of θ) and $(T_0, E_0, I_0) = (1, 0, 0)$, $T(t) = 0$ for $t < 0$. Notice the tumor resting period in $t \in [120, 160]$ (right zoom for $\theta \in \{1, 1.5, 2\}$), the length of which depends on θ, is the one in witch the hybrid system probabilistically switches to the null attractor for T. On the x-axis days are represented, on the y-axis number of cells.

In both cases one may observe a 'tumor resting' interval $t \in [120, 160]$, where the tumor size is very small, and whose length depends on θ. OF course, also the minimal value of T depends on θ. For example, for $\theta = 2$ the predicted minimum tumor size is smaller than one cell, ad remains very small for many days, and for $\theta = 1.5$ this minumum vaue is 10 cells about.

In this resting period, instead, the hybrid system stochastically switches to $T = 0$, which is an adsorbing state. As in [14], this behavior confirms the importance of adopting the hybrid modeling of the tumor-immune system interplay.

5. **Conclusions.** In this paper we study the effect of Erlang-distributed time delay in effectors recruitment in a tumor–Immune system interplay hybrid model. Namely, in our simulations we considered the exponential and the strong kernel. The model, suitably extending a well-known mean-field model [55], was proved to be more informative to forecast onco-suppression by the Immune system [14] as a conjunction of strong intrinsic tendency of the tumor-Immune system to oscillate, which was also evidenced by the deterministic models [55, 23], with the intrinsic stochastic nature of the studied phenomena, fundamental when the tumor cells and/or the Immune system effectors reach low numbers.

Of course, modeling tumors, and in particular tumor–Immune system interplay, requires considering manifold cellular types and chemical entities at multiple temporal and spatial scales. As a consequence, tumor growth and antitumor therapies are ideal objects of hybrid modeling, as we have shown in [14, 27]. We stress here that hybrid models may have various degrees of detail, and that in [14, 27] we focused on a relatively simple, but effective, approach where spatial scale is not directly represented. However, note that a direct and fine inclusion of the spatial scale and of some complex phenomena such as differentiation and activation of T-lymphocytes is currently unfeasible, also for a lack of systematic data [12]. A way to indirectly consider spatial chemical transportation of intercellular signals, as well as of composite phenomena, e.g. cellular differentiation and division, is represented by the inclusion of delays in the hybrid model of [14]. The lags, indeed, heuristically allow to represent the influence of the above phenomena, and in particular to model the fact that the influence of tumor on effectors recruitment and proliferation is not instantaneous. The modeling of the delays is by no means simple, and here we adopted the approach of representing them with suitable probability densities, i.e. the Erlang functions successfully adopted in many fields of theoretical biology.

By the use of supplementary variables we contextualized this model within the framework of Stochastic Hybrid Automata, so to give it a semantics in terms of Piecewise Deterministic Markov Processes [32]. This is a similar approach to that followed in [14], but for a bigger system extended with Erlang-distributed delays. We present a novel algorithm to simulate this extended hybrid model and we analyze it under various configurations. Since an analytical study was not feasible, we performed intensive numerical simulations by adopting the realistic constellation of parameters also employed in [14], for both considered kernels.

First, for both kernels and values of the antigenicity parameter c that does not induce stochastic oscillations in absence of delay, we quantified the effects of various average delays on tumor mass growth. Also, we determined probability distributions of the tumor self-extinction time, when possible. Then, under these configurations we also performed a parametric sensitivity analysis technique, in order to link the tumor growth to the delay amplitude θ.

Finally, for values of c inducing an oscillatory regime in absence of delay, our simulations showed that the presence of delays may induce an unexpected self-suppression of the tumor. In other and more mathematical words, our simulations proved the existence of an oscillation/suppression transition, which was not present in the non-delayed hybrid model. Note that, in line with the general definition of Zeeman for random continuous dynamical systems [74], the phenomenon here observed is a stochastic bifurcation since here a changes in the characteristics of the density for varying delays. In other words, θ can be considered as the 'tunable' bifurcation parameter.

Summarizing, despite our model is to some extent a toy-representation of the real tumor–Immune system interplay, nevertheless it can provide useful and novel insights on the manifold possible outcomes of this fundamental and complex interaction.

We are currently investigating also the case of the presence of a constant delay, i.e. a Dirac kernel, in effectors recruitment [15]. Note that the SHA here proposed is deeply different from the one describing the system with Dirac kernel [15]. In fact, although the constant lag structure may appear simpler than the one here considered, in reality the Dirac delay kernel is a *generalized* function, i.e. a more

complex mathematical entity. It follows that in order to account for equation (1) in [15] a clock structure of a Generalized Semi-Markov Process (GSMP) [46] has to be superimposed to the SHA for the delay-free case [1]

As far as future works are concerned, the inclusion of active and passive immunotherapies, as those modeled in [27], and of immuno-editing mechanisms, as those modeled in [29, 30], would be a first important step. Moreover, the basic model [55] itself needs some improvements. For example, instead of a linear antigenic effect $cT(t)$ it might be more appropriate to consider a saturating antigenic effect triggering the Immune system. Concerning instead the type of delays considered, more complex integro-differential delay kernels could be used, e.g. power-law fading kernels. Finally, the mathematical characterization of hybrid automata with delays seems to be missing, thus suggesting possible extensions to the hybrid automata theory, along with their analysis techniques.

Acknowledgments. A.G. acknowledges Regione Lombardia, project RetroNet, grant 12-4-5148000-40; U.A 053, and NEDD for financial support of this work. A.d'O. acknowledges the support by the project "p-medicine - From data sharing and integration via VPH models to personalized medicine", a 4-year Integrated Project co-funded under the EC 7th Framework Programme.

REFERENCES

[1] S. A. Agarwala, "New Applications of Cancer Immunotherapy," S. A. Agarwala (Guest Editor), Sem. Onc., Special Issue 29-3 Suppl. 7. 2003.

[2] R. Barbuti, G. Caravagna, A. Maggiolo-Schettini and P. Milazzo, *Delay stochastic simulation of biological systems: A purely delayed approach*, C.Priami et al.(Eds.): Trans. Comp. Sys. Bio. XIII, LNBI, **6575** (2011), 61–84.

[3] M. Barrio, K. Burrage, A. Leier and T. Tian, *Oscillatory regulation of Hes1: Discrete stochastic delay modelling and simulation*, PLoS Comp. Bio., (9), **2** (2006).

[4] N. Bellomo and G. Forni, *Complex multicellular systems and Immune competition: New paradigms looking for a mathematical theory*, Curr. Top. Dev. Bio., **81** (2008), 485–502.

[5] E. Beretta, V. Capasso and F. Rinaldi, *Global stability results for a generalized Lotka-Volterra system with distributed delays*, J. Math. Bio., **26** (1988), 661–688.

[6] I. Bleumer, E. Oosterwijk, P. de Mulder and P. F. Mulders, *Immunotherapy for renal cell carcinoma*, Europ. Urol., **44** (2003), 65–75.

[7] N. Blumberg, C. Chuang-Stein and J. M. Heal, *The relationship of blood transfusion, tumor staging and cancer recurrence*, Transf., **30** (1990), 291–294.

[8] K. B. Blyuss and Y. N. Kyrychko, *Stability and bifurcations in an epidemic model with varying immunity period*, Bull. Math. Bio., **72** (2010), 490–505.

[9] L. Bortolussi, *Automata and (stochastic) programs. The hybrid automata lattice of a stochastic program*, J. Log. Comp., (2011).

[10] L. Bortolussi and A. Policriti, *The importance of being (a little bit) discrete*, ENTCS, **229** (2009), 75–92.

[11] M. Bravetti and R. Gorrieri, *The theory of interactive generalized semi-Markov processes*, Theoret. Comp. Sci., **282** (2002), 5–32.

[12] N. Burić and D. Todorović, *Dynamics of delay-differential equations modelling immunology of tumor growth*, Cha. Sol. Fract., **13** (2002), 645–655.

[13] G. Caravagna, "Formal Modeling and Simulation of Biological Systems With Delays," Ph.D. Thesis, Università di Pisa. 2011.

[14] G. Caravagna, A. d'Onofrio, P. Milazzo and R. Barbuti, *Antitumour Immune surveillance through stochastic oscillations*, J. Th. Biology, **265** (2010), 336–345.

[1] It is shown in [16, 13] that these processes underly Gillespie-like [45] chemically reacting systems with deterministic constant delays, those indeed used in [15].This further structure was not necessary here, as we showed.

[15] G. Caravagna, A. Graudenzi, M.Antoniotti, G. Mauri and A. d'Onofrio, *Effects of delayed Immune-response in tumor Immune-system interplay*, Proc. of the First Int. Work. on Hybrid Systems and Biology (HSB), EPTCS, **92** (2012), 106–121.
[16] G. Caravagna and J. Hillston, *Bio-PEPAd: A non-Markovian extension of Bio-PEPA*, Th. Comp. Sc., **419** (2012), 26–49.
[17] G. Caravagna, G. Mauri and A. d'Onofrio, *The interplay of intrinsic and extrinsic bounded noises in genetic networks*, Submitted. Preprint at http://arxiv.org/abs/1206.1098.
[18] V. Costanza and J. H. Seinfeld, *Stochastic sensitivity analysis in chemical kinetics*, J. Chem. Phys., **74** (1981), 3852–3858.
[19] D. R. Cox, *The analysis of non-Markovian stochastic processes by the inclusion of supplementary variables*, Proc. Cambridge Phil. Soc., **51** (1955), 433–440.
[20] F. Crauste, *Stability and hopf bifurcation for a first-order delay differential equation with distributed delay*, in "Complex Time-Delay Systems: Theory and Applications" (ed. F.M. Atay), Springer, (2010), 263–296.
[21] P. R. D'Argenio, J.-P. Katoen and E. Brinksma, *A stochastic automata model and its algebraic approach*, Proc. 5th Int. Workshop on Process Algebra and Performance Modeling, CTIT technical reports series 97–14, University of Twente, 1–16. (1997).
[22] C. Damiani and P. Lecca, *A novel method for parameter sensitivity analysis of stochastic complex systems*, in "Publication on The Microsoft Research – University of Trento Centre for Computational and Systems Biology Technical Reports" 2012. http://www.cosbi.eu/index.php/research/publications?abstract=6546.
[23] A. d'Onofrio, *Tumor-Immune system interaction: modeling the tumor-stimulated proliferation of effectors and immunotherapy*, Math. Mod. Meth. App. Sci., **16** (2006), 1375–1401.
[24] A. d'Onofrio, *Tumor evasion from Immune system control: Strategies of a MISS to become a MASS*, Ch. Sol. Fract., **31** (2007), 261–268.
[25] A. d'Onofrio and P. Manfredi, *Information-related changes in contact patterns may trigger oscillations in the endemic prevalence of infectious diseases*, J. Th. Bio., **256** (2009), 473–478.
[26] A. d'Onofrio, *On the interaction between the Immune system and an exponentially replicating pathogen*, Math. Biosc. Eng., **7** (2010), 579–602.
[27] A. d'Onofrio, G. Caravagna and R. Barbuti, *Fine-tuning anti-tumor immunotherapies via stochastic simulations*, BMC Bioinformatics, (4), **13** (2012).
[28] A. d'Onofrio, *Tumour evasion from Immune system control as bounded-noise induced transition*, Phys. Rev. E, **81** (2010), Art. n. 021923.
[29] A. d'Onofrio and A. Ciancio, *A simple biophysical model of tumor evasion form Immune control*, Phys. Rev. E, **84** (2011), Art. n. 031910.
[30] M. Al Tameemi, M. Chaplain and A. d'Onofrio, *Evasion of tumours from the control of the Immune system: consequences of brief encounters*, Biology Direct, in press. 2012.
[31] A. d'Onofrio, F. Gatti, P. Cerrai and L. Freschi, *Delay-induced oscillatory dynamics of Tumor-Immune system interaction*, Math. Comp. Mod., **51** (2010), 572–591.
[32] H. H. A. Davis, *Piecewise deterministic Markov processes: a general class of non-diffusion stochastic models*, J. Roy. Stat. So. Series B, **46** (1984), 353–388.
[33] R. J. DeBoer, P. Hogeweg, F. Hub, J. Dullens, R. A. DeWeger and W. DenOtter, *Macrophage T Lymphocyte interactions in the anti-tumor Immune response: A mathematical model*, J. Immunol., **134** (1985), 2748–2758.
[34] L. G. De Pillis, A. E. Radunskaya and C. L. Wiseman, *A validated mathematical model of cell-mediated Immune response to tumor growth*, Cancer Res., **65** (2005), 7950–7958.
[35] V. T. De Vito Jr., J. Hellman and S. A. Rosenberg, "Cancer: Principles and Practice of Oncology," J. P. Lippincott. 2005.
[36] G. P. Dunn, L. J. Old and R. D. Schreiber, *The three ES of Cancer Immunoediting*, Ann. Rev. of Immun., **22** (2004), 322–360.
[37] P. Ehrlich, *Ueber den jetzigen Stand der Karzinomforschung*, Ned. Tijdschr. Geneeskd., **5** (1909), 273–290.
[38] H. Enderling, L. Hlatky and P. Hahnfeldt, *Immunoediting: Evidence of the multifaceted role of the immune system in self-metastatic tumor growth*, Theoretical Biology and Medical Modelling, **9** (2012), Art.n. 31.
[39] M. Farkas, "Periodic Motions," Springer-Verlag, Berlin and New York, 1994.
[40] P. Feng, *Dynamics of a segmentation clock model with discrete and distributed delays*, Int. J. Biomath., **3** (2010), 1–18.

[41] M. Galach, *Dynamics of the tumour-Immune system competition: The effect of time delay*, Int. J. App. Math. and Comp. Sci., **13** (2003), 395–406.
[42] C. W. Gardiner, "Handbook of Stochastic Methods," (2nd edition). Springer. 1985.
[43] R. Gatti, et al., *Cyclic Leukocytosis in Chronic Myelogenous Leukemia: New Perspectives on Pathogenesis and Therapy*, Blood, **41** (1973), 771–783.
[44] D. T. Gillespie, *A general method for numerically simulating the stochastic time evolution of coupled chemical reactions*, J. of Comp. Phys., **22** (1976), 403–434.
[45] D. T. Gillespie, *Exact stochastic simulation of coupled chemical reactions*, J. of Phys. Chem., **81** (1977), 2340–2361.
[46] P. W. Glynn, *On the role of generalized semi-markov processes in simulation output analysis*, Proc. of the 15th conference on Winter simulation, **1** (1983), 39–44.
[47] R. Gunawan, Y. Cao, L. Petzold and F. J. Doyle III, *Sensitivity analysis of discrete stochastic systems*, Biophys. J., **88** (2005), 2530–2540.
[48] S. A. Gourley and S.Ruan, *Dynamics of the diffusive Nicholson blowflies equation with distributed delay*, Proc. Roy. Soc. Edinburgh A, **130** (2000), 1275–1291.
[49] Y. Han and Y. Song, *Stability and Hopf bifurcation in a three-neuron unidirectional ring with distributed delays*, Nonlin. Dyn., **69** (2011), 357–370.
[50] R. Jessop, "Stability and Hopf Bifurcation Analysis of Hopfield Neural Networks with a General Distribution of Delays," University of Waterloo, available at http://uwspace.uwaterloo.ca/bitstream/10012/6403/1/Jessop_Raluca.pdf. 2011.
[51] C. H. June, *Adoptive T cell therapy for cancer in the clinic*, J. Clin. Invest., **117** (2007), 1466–1476.
[52] J. M. Kaminski, J. B. Summers, M. B. Ward, M. R. Huber and B. Minev, *Immunotherapy and prostate cancer*, Canc. Treat. Rev., **29** (2004), 199–209.
[53] B. J. Kennedy, *Cyclic leukocyte oscillations in chronic myelogenous leukemia during hydroxyurea therapy*, Blood, **35** (1970), 751–760.
[54] D. Kirschner, J. C. Arciero and T. L. Jackson, *A mathematical model of tumor-Immune evasion and siRNA treatment*, Discr. Cont. Dyn. Systems, **4** (2004), 39–58.
[55] D. Kirschner and J. C. Panetta, *Modeling immunotherapy of the tumor-Immune interaction*, J. Math. Biol., **37** (1998), 235–252.
[56] Y. Kuang, "Delay Differential Equations with Applications in Population Dynamics," Academic Press, 1993.
[57] Y. Kuang, *Delay differential equations*, Sourcebook in Theoretical Ecology, Hastings and Gross ed., University of California Press, 2011.
[58] K. A. Kuznetsov and G. D. Knott, *Modeling tumor regrowth and immunotherapy*, Math. Comp. Mod., **33** (2001).
[59] V. A. Kuznetsov, I. A. Makalkin, M. A. Taylor and A. S. Perelson, *Nonlinear dynamics of immunogenic tumors: Parameter estimation and global bifurcation analysis*, Bull. Math. Biol., **56** (1994), 295–321.
[60] M. C. Mackey and L. Glass, *Oscillation and chaos in physiological control systems*, Sc., **197** (1977), 287–289.
[61] R. M. C. May and A. R. McLean, "Theoretical Ecology: Principles and Applications," Oxford University Press, USA. 2007.
[62] B. C. Mehta and M. B. Agarwal, *Cyclic oscillations in leukocyte count in chronic myeloid leukemia*, A. Hem. **63** (1980), 68–70.
[63] J. D. Murray, "Mathematical Biology," third edition, Springer Verlag, Heidelberg, 2003.
[64] D. Pardoll, *Does the Immune system see tumours as foreign or self?*, Ann. Rev. Immun., **21** (2003), 807–839.
[65] D. Rodriguez-Perez, O. Sotolongo-Grau, R. Espinosa, R. O. Sotolongo-Costa, J. A. Santos Miranda and J. C. Antoranz, *Assessment of cancer immunotherapy outcome in terms of the Immune response time features*, Math. Med. and Bio., **24** (2007), 287–300.
[66] P. Martin, S. Martin, P. Burton and I. Roitt, "Roitt's Essential Immunology," Wiley-Blackwell, 2011.
[67] S. Ruan, *Delay differential Eequation in single species dynamics*, in "NATO Science Series" (eds. O. Arino, M.L. Hbid and E. Ait Dads), **1** (205), Delay Differential Equations and Applications IV, 477–517.
[68] A. Sohrabi, J. Sandoz, J. S. Spratt and H. C. Polk, *Recurrence of breast cancer: Obesity, tumor size, and axillary lymph node metastases*, JAMA, **244** (1980), 264–265.

[69] H. Tsao, A. B. Cosimi and A. J. Sober, *Ultra-late recurrence (15 years or longer) of cutaneous melanoma*, Cancer, **79** (1997), 2361–2370.
[70] A. P. Vicari, G. Caux and G. Trinchieri, *Tumor escape from Immune surveillance through dendritic cell inactivation*, Sem. Canc. Biol., **2** (2002), 33–42.
[71] M. Villasana and A. Radunskaya, *A delay differential equation model for tumour growth*, J. of Math. Bio., **47** (2003), 270–294.
[72] H. Vodopick, E. M. Rupp, C. L. Edwards, F. A. Goswitz and J. J. Beauchamp, *Spontaneous cyclic leukocytosis and thrombocytosis in chronic granulocytic leukemia*, New Engl. J. of Med., **286**(1972), 284–290.
[73] T. L. Whiteside, *Tumor-induced death of Immune cells: Its mechanisms and consequences*, Sem. Canc. Biol., **12** (2002), 43–50.
[74] E. C. Zeeman, *Stability of dynamical systems*, Nonlin., **1** (1988), 115–155.
[75] C. H. Zhang and Y. Xiang-Ping, *Stability and Hopf bifurcations in a delayed predator-prey system with a distributed delay*, Int. J. Bifur. Chaos Appl. Sci. Eng., **19** (2009), 2283–2294.

Appendix A. **Model simulation.** Algorithm 1, works by determining, at each iteration, both the exit time from the current mode and the next mode. So, when at time t_q the automaton enters a mode q, the exit time τ (step 4) is determined by the parallel solution of $I(t)$ and $Z(t)$, $t \geq t_q$, and $\mathcal{P}_q[\tau]$ as triggered by the jump rates $a_{j,q}(t)$. As explained in Section 3, samples from $\mathcal{P}_q[\tau]$ are obtained by the unit-rate Poisson transformation (step 4) in equation (12). It is worth nothing that for a time-constant propensity functions it holds the simplified equation

$$\int_0^\tau a_{i,q}(t_q + t)dt = \tau a_{i,q}(t_q)$$

so formula (12) rewrites as

$$\sum_{i\in\{1,2,3,5\}} \tau a_{i,q}(t_q) + \sum_{i\in\{4,6\}} \int_0^\tau a_{i,q}(t_q + t)dt = \ln\left(\frac{1}{r_1}\right).$$

Further simplifications are indeed possible, in fact

$$\int_0^\tau a_{4,q}(t_q + t)dt = \frac{p_I q_E}{\alpha}\left[\tau\mu_I\alpha + g_E \ln\left(\frac{g_E + I_q}{-B_q + e^{\tau\mu_I}\alpha + I_q}\right)\right] \tag{16}$$
$$\int_0^\tau a_{6,q}(t_q + t)dt = c\,\mathbf{ph}\,q_T\tau + c\mathbf{p}A^{-1}e^{A\tau}(\mathbf{w}_q - q_T\mathbf{h})$$

with $\alpha = B_q + g_E$. The top equation is first given in [14]. Note that if the average delay θ is very small it is $\int_0^\tau a_{6,q}(t_q + t)dt \approx c\,\mathbf{ph}\,q_T\tau$, as expected.

The algorithm performs a realization of the process starting from an initial configuration $(T_0, E_0, I_0, \mathbf{w}_0)$ but, if the history of $T(t)$ is known for $t_{\text{birth}} < t < 0$, where $t_{\text{birth}} < 0$ is the birth date of the host organism, an extended initial condition for $\mathbf{W}$ could be defined as

$$\mathbf{W}(0) = \int_{t_{\text{birth}}}^0 e^{Ax}T(x)dx\,.$$

Appendix B. **Weak and strong kernels.** The *"weak"* and *"strong"* delay kernels [39] defined in Section 3.1 correspond to $M = 1$ and $M = 2$, respectively. Since if $M = 1$ then $a = 1/\theta$, whereas if $M = 2$ then $a = 2/\theta$, we have that when $M = 1$, i.e. $Z(t) = W(t)$, the generic equation (16) rewrites as

$$\int_0^\tau a_{6,q}(t_q + t)dt = c\left[q_T\tau + \alpha\frac{w_q - q_T}{a}\right]$$

with $W(t_q) = w_q$ and $\alpha = 1 - e^{-a\tau}$.

Differently, if $M = 2$, i.e. $\mathbf{W}(t) = (W_1(t), W_2(t))$ and $Z(t) = W_2(t)$, then

$$\int_0^\tau a_{6,q}(t_q + t)dt = c\left[q_T\tau + \alpha\frac{w_{2,q} - q_T}{a} + (w_{1,q} - q_T)\left(-\tau e^{-a\tau} + \frac{\alpha}{a}\right)\right]$$

with $\mathbf{W}(t_q) = (w_{1,q}, w_{2,q})$ and $\alpha = 1 - e^{-a\tau}$.

Finally, note that for $M = 2$, when the SHA jumps from $\mathbf{W}(t_q) = (w_{1,q}, w_{2,q})$ to $\mathbf{W}(t_{q'}) = (w_{1,q'}, w_{2,q'})$ it holds

$$\begin{aligned} w_{1,q'} &= q_T + e^{-a\Delta_t}(w_{1,q} - q_T) \\ w_{2,q'} &= q_T + e^{-a\Delta_t}\left[(w_{2,q} - q_T) + a\Delta_t(w_{1,q} - q_T)\right] \end{aligned}$$

with $\Delta_t = t_{q'} - t_q$. These last simplified equations can be used while evaluating steps 4 and 5 of Algorithm 1.

Received July 2, 2012; Accepted September 25, 2012.

E-mail address: giulio.caravagna@unimib.it
E-mail address: alex.graudenzi@unimib.it
E-mail address: alberto.donofrio@ieo.eu